Tuning the magnetic anisotropy in CeRhIn$_5$ via Gd substitution

P. F. S. Rosa, L. M. Faust, E. D. Bauer, and J. D. Thompson

Los Alamos National Laboratory, Los Alamos, New Mexico 87545, USA

In strongly correlated materials, the presence of defects may fundamentally affect both macroscopic and microscopic properties of the system. Here we investigate the effect of Gd substitution in the Kondo antiferromagnet CeRhIn$_5$. At a concentration of only 11% Gd, the magnetic anisotropy of CeRhIn$_5$ is drastically reduced at high temperatures, whereas its antiferromagnetic transition, $T_N^{Ce} = 3.8$ K, is linearly suppressed with Gd at low temperatures. The extrapolation of T_N^{Ce} to zero temperature occurs at a critical concentration of $x_c \sim 0.63$, which is above the two-dimensional percolation limit found in Ce$_{1-x}$La$_x$RhIn$_5$ ($x_c \sim 0.4$), but very close to the three-dimensional percolation limit found in Gd$_{1-x}$La$_x$RhIn$_5$ and Ce$_{1-x}$La$_x$In$_3$ ($x_c \sim 0.65$), in agreement with the more isotropic magnetic response.

I. INTRODUCTION

The controlled introduction of disorder in a system is a powerful tool not only to probe its fundamental properties but also to induce novel emergent phenomena. For instance, disorder is a necessary condition to explain the emergence of quantized steps in the quantum integer Hall effect in noninteracting electronic systems [1]. Additionally, the response of superconductors to impurities provides valuable information on the superconducting gap structure and is well described by the Abrikosov-Gork'ov (AG) theory for noninteracting systems [2,3].

When electron-electron interactions become important, however, the theoretical frameworks mentioned above break down. In the case of the quantum Hall effect, fractional quantized steps are observed in interacting systems [4]. In the case of superconductivity, recent experiments reveal unexpected effects when magnetic impurities are introduced into correlated superconductors with strong electron-electron interactions among d or f electrons. For instance, tiny amounts of Mn substitution in superconducting LaFeAsO$_{1-x}$F$_x$ have a poisoning effect on superconductivity. This effect is strongly enhanced when compared to the AG theory owing to electronic correlations [5,6]. Moreover, when 5% Nd is introduced into heavy-fermion superconductors CeCoIn$_5$ and CeRhIn$_5$ under pressure, an unprecedented spin-density-wave instability at zero magnetic field emerges inside the superconducting dome [7–9].

In spite of the growing understanding of the unexpected effects of magnetic impurities in unconventional superconductors, little is known about the role of magnetic impurities on the bordering antiferromagnetic ground state of these materials. What is well known is that, when a few parts per million of magnetic impurities are added to a *nonmagnetic* host, the electrical resistance of the host rises logarithmically at a material-specific Kondo impurity temperature T_K [10]. This so-called single-ion Kondo effect reflects the incoherent scattering of conduction electrons by the magnetic impurities introduced into the host [11]. When both the metal host and the impurities are magnetic, however, an additional interaction between the host ions and the magnetic impurities may appear and the resulting ground state is rather unpredictable. In this regard, the highly tunable and exceptionally impurity-free antiferromagnet metal CeRhIn$_5$ provides an ideal platform for this investigation [12].

When nonmagnetic La ions replace Ce ions in the tetragonal Kondo lattice Ce$_{1-x}$La$_x$RhIn$_5$, a "Kondo hole" is created such that the antiferromagnetic transition temperature in pure CeRhIn$_5$ ($T_N^{Ce} = 3.8$ K) decreases linearly with La and extrapolates to $T = 0$ at a critical La concentration of $x_c \sim 40\%$ [13,14]. Interestingly, this critical concentration coincides with the percolation limit of a two-dimensional (2D) square lattice on which the La/Ce ions sit. In contrast, magnetic Nd^{3+} substitution in CeRhIn$_5$ shows that the Nd^{3+} ions act as an unusual Kondo hole [15]. Although T_N also decreases linearly with Nd, it extrapolates to zero temperature at $x_c \sim 30\%$, indicating that there is an additional mechanism frustrating T_N besides dilution of the Ce^{3+} lattice. It has been argued that this mechanism is the magnetic frustration due to the different spin configurations of CeRhIn$_5$, which has easy c-axis magnetization but in-plane ordered moments [16], and NdRhIn$_5$, which has Ising spins along the c axis [17]. Because the magnetic moments of Ce and Nd are orthogonal, Nd ions behave, to a first approximation, as free paramagnetic impurities.

The question, however, of how an antiferromagnetic Kondo lattice host and magnetic impurities interact remains unanswered, and the introduction of magnetic impurities with in-plane moments provides a route to understand this problem. In this work, we report the study of Ce$_{1-x}$Gd$_x$RhIn$_5$ by means of x-ray diffraction, microprobe, magnetization, and heat capacity measurements. Our data show that the Ce-derived antiferromagnetic (AFM) ordering temperature of Ce$_{1-x}$Gd$_x$RhIn$_5$ decreases linearly with Gd concentration, x_{Gd}, and extrapolates to zero at a critical Gd concentration of $x_c \sim 63\%$. In the dilute regime, Gd^{3+} ions do not behave as free paramagnetic impurities, and drastically reduce the magnetic anisotropy of Kondo CeRhIn$_5$ at high temperatures. Although x_c is above the 2D percolation limit found previously in Ce$_{1-x}$La$_x$RhIn$_5$ ($x_c \sim 0.4$) [13], it is surprisingly close to the three-dimensional (3D) percolation limit found in Gd$_{1-x}$La$_x$RhIn$_5$ and cubic Ce$_{1-x}$La$_x$In$_3$ ($x_c \sim 0.65$) [18], in agreement with the more isotropic magnetic response.

II. EXPERIMENTAL DETAILS

Single crystalline samples of $Ce_{1-x}Gd_xRhIn_5$ were grown by the indium-flux technique. The crystallographic structure was verified by x-ray powder diffraction at room temperature. Magnetization measurements were performed using a commercial superconducting quantum interference device and the specific heat was measured using a commercial small mass calorimeter that employs a quasiadiabatic thermal relaxation technique. The samples reported here were characterized by elemental analysis using a commercial energy dispersive spectroscopy (EDS) microprobe.

III. RESULTS and DISCUSSION

According to the x-ray powder diffraction patterns, all members of the series $Ce_{1-x}Gd_xRhIn_5$ crystallize in the tetragonal $HoCoGa_5$ structure and no additional peaks are observed. Figure 1 shows the evolution of the lattice parameters in the series as a function of the actual Gd concentration obtained by EDS (x_{EDS}). The smooth and monotonic relationship between the lattice parameters and x_{EDS} indicates that Gd is being incorporated in the lattice according to Vegard's law. The standard deviation of the Gd concentration obtained by EDS is 1–2 %, indicating that Gd substitutes Ce homogeneously instead of producing an intergrowth of $GdRhIn_5$. Herein, we will refer to the actual EDS concentration. We note, however, that there is a region of insolubility between the two end compounds. This region, ranging from about 12% to 29% Gd, is shown by the dashed area in Fig. 1.

The decrease in the volume of the unit cell with x suggests that Gd substitution is responsible for applying positive chemical pressure, similar to Nd substitution. Using the bulk modulus of $CeRhIn_5$, we estimate that a rigid shift of the lattice parameters from $CeRhIn_5$ to $Ce_{0.966}Gd_{0.034}RhIn_5$ corresponds to $\Delta P = 1$ kbar of applied pressure. From the phase diagram of $CeRhIn_5$ under pressure [19], this ΔP would correspond to an increase of T_N by $\sim$0.1 K. We will see below that the AFM order due to Ce $4f$ electrons actually is suppressed at small
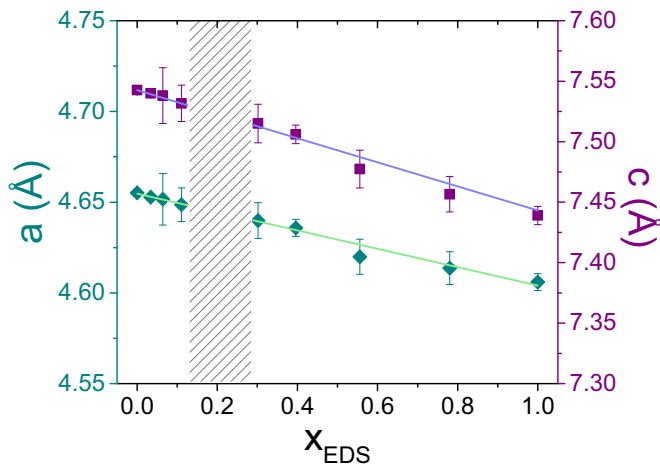

FIG. 1. Tetragonal lattice parameters as a function of the actual concentration measured by EDS, x_{EDS}, along the series $Ce_{1-x}Gd_xRhIn_5$.
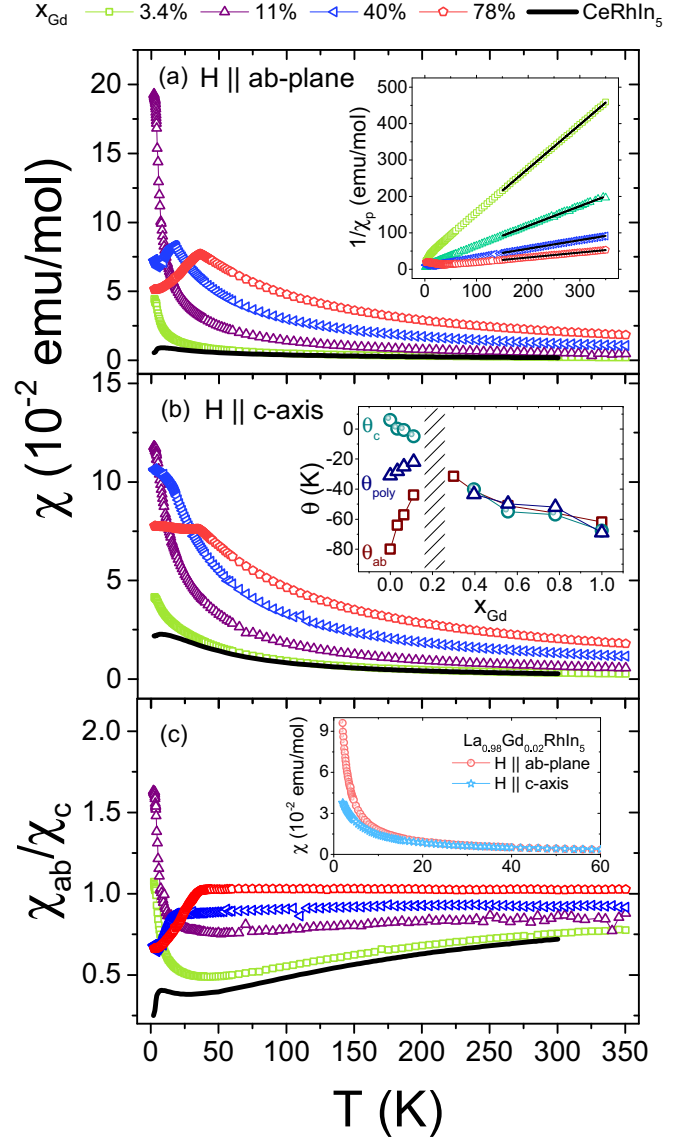

FIG. 2. (a) Temperature dependence of the magnetic susceptibility, $\chi_{ab}(T)$, of representative samples in the $Ce_{1-x}Gd_xRhIn_5$ series in a field of 1 kOe applied along the ab plane. Inset shows the inverse susceptibility of the polycrystalline average. Solid lines are linear fits to the data. (b) Temperature dependence of the magnetic susceptibility, $\chi_c(T)$, in a field of 1 kOe applied along the c axis. Inset shows the Curie-Weiss temperature, θ, for all compositions of $Ce_{1-x}Gd_xRhIn_5$. (c) Temperature dependence of the ratio between $\chi_{ab}(T)$ and $\chi_c(T)$. Inset shows the anisotropic magnetic susceptibility of $La_{0.98}Gd_{0.02}RhIn_5$ at 1 kOe.

Gd concentrations, indicating that chemical pressure is not the main tuning parameter determining T_N.

Figures 2(a) and 2(b) show the temperature dependence of the magnetic susceptibility, $\chi(T)$, for representative samples in the series $Ce_{1-x}Gd_xRhIn_5$ when a field of 1 kOe is applied along the ab plane, $\chi_{ab}(T)$, and c axis, $\chi_c(T)$, respectively. Evidence of T_N in these data changes from a maximum in $d\chi/dT$ at 3.8 K in $CeRhIn_5$ to a local maximum in $\chi(T)$ for low Gd concentrations. This result suggests that Gd substitution is changing the effective exchange interaction

between Ce $4f$ electrons, as also observed in the case of nonmagnetic La substitution [13]. Further, even at the lowest Gd concentration, the calculated paramagnetic (Curie) contribution from free Gd^{3+} ions would be larger than the measured $\chi(T)$. This in turn indicates that Gd^{3+} ions are not free paramagnetic impurities, in contrast with the case of magnetic Nd substitution. This difference is likely due to the different spin configurations of Nd and Gd. Nd^{3+} spins are Ising-like and point along the c axis [17], whereas Gd^{3+} spins are Heisenberg-like and lie in the ab plane [20]. Therefore, one would naively expect a larger interaction between Gd^{3+} impurities and the lattice of Ce^{3+} spins, which also lie in the ab plane. For Gd concentrations to 11%, the AFM order arising from the Ce lattice decreases smoothly. At higher x_{Gd}, however, the transition temperature starts to increase again, suggesting that the AFM order due to Gd ions starts to develop at T_N^{Gd}. For higher Gd concentrations, both $\chi_c(T)$ and $\chi_{ab}(T)$ show AFM behavior of a typical isotropic local moment system with hard axis along the c axis. We will return to this analysis when discussing the phase diagram in Fig. 4.

The polycrystalline average of the data can be fit to a Curie-Weiss law, and the obtained paramagnetic Curie-Weiss temperatures are shown in the inset of Fig. 2(a), as well as θ_c and θ_{ab}. In a molecular field approximation, θ_{poly} is proportional to the effective exchange interaction, J, between rare-earth ions. The fact that θ_{poly} is negative is in agreement with the AFM correlations found in the series. A reduction of $|\theta_{poly}|$ is observed as a function of Gd substitution up to $x_{Gd} = 0.11$, suggesting that the effective J_{RKKY} between Ce $4f$ electrons also decreases in this range. As a consequence, this reduction in J would be expected to cause a decrease in T_N. As we will come to later, the experimental data do agree with this expectation. Further, $|\theta_{poly}|$ starts to increase again above $x_{Gd} = 0.11$, indicating that the exchange interaction among Gd $4f$ electrons becomes increasingly important. In fact, T_N^{Gd} experimentally increases in this concentration range.

Importantly, besides Ruderman-Kittel-Kasuya-Yosida (RKKY) and Kondo interactions, crystalline electric-field (CEF) effects may also set a relevant energy scale in $4f$ systems. From a high-temperature expansion of $\chi(T)$ one can calculate the main tetragonal CEF parameter, $B_2^0 \propto (\theta_{ab} - \theta_c)$, which decreases systematically at low Gd concentrations. This strongly indicates that CEF effects are responsible for the decrease in the high-temperature magnetic anisotropy in this concentration range as shown in the inset of Fig. 2(b). The ratio χ_{ab}/χ_c further illustrates that the magnetic susceptibility is becoming more isotropic with Gd substitution at high temperatures [Fig. 2(c)]. Above $x_{Gd} = 0.11$, B_2^0 is zero owing to the fact that Gd^{3+} is an S ion and CEF effects are second-order effects. This result is in agreement with the fact that the AFM order is due to the Gd sublattice above $x_{Gd} = 0.11$. We note that, at low temperatures and low Gd concentrations, an anisotropic Curie tail appears as illustrated in the inset of Fig. 2(c) for La$_{0.98}$Gd$_{0.02}$RhIn$_5$.

In a Kondo lattice such as CeRhIn$_5$, θ_{poly} also includes the AFM Kondo exchange that tends to reduce T_N relative to that expected solely from the indirect RKKY interaction [21]. Because there is no Kondo effect in GdRhIn$_5$, the variation in θ_{poly} with x_{Gd} implies a suppression of the Kondo contribution and increased dominance of the RKKY interaction. As
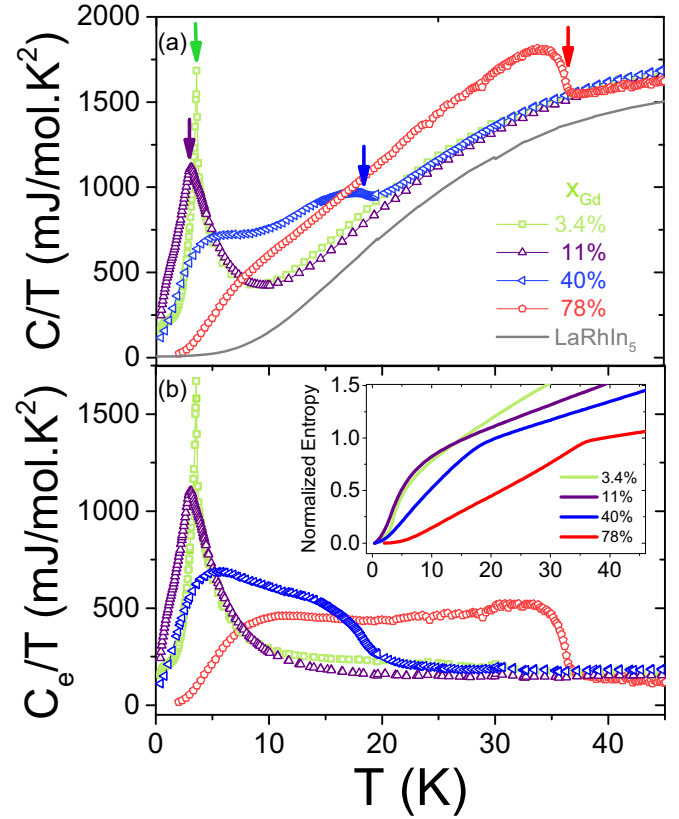

FIG. 3. (a) Temperature dependence of the specific heat, C/T, of LaRhIn$_5$, CeRhIn$_5$, and representative samples of the series Ce$_{1-x}$Gd$_x$RhIn$_5$. (b) Magnetic contribution to the specific heat, C_{mag}/T, as a function of temperature. Inset shows the entropy normalized by $(1 - x_{Gd})R \ln 2 + x_{Gd}R \ln 8$.

illustrated in the inset of Fig. 2(b), $|\theta_{poly}|$ does decrease at low Gd concentration, suggesting that contributions to $|\theta_{poly}|$ from Kondo interactions are also reduced in this concentration range. If Kondo interactions dominated the magnitude of $T_N(x)$, one might expect T_N to increase initially as Gd replaces Ce but this is not observed experimentally. We therefore conclude that the Kondo effect is not the dominant parameter determining T_N and θ_{poly}.

Figure 3(a) shows the temperature dependence of the heat capacity over temperature, C/T, for four representative Gd concentrations and LaRhIn$_5$, the nonmagnetic member. The sharp peak of Ce$_{0.966}$Gd$_{0.034}$RhIn$_5$ at $T_N = 3.57$ K (marked by a green arrow) is very similar to the response of pure CeRhIn$_5$ ($T_N = 3.8$ K). At $x_{Nd} = 0.11$, the transition at T_N starts to broaden and, as x_{Gd} is further increased, there is an enhancement of T_N in agreement with $\chi(T)$ data.

Figure 3(b) shows the electronic contribution to the heat capacity, C_e/T, determined by subtracting the phonon specific heat of LaRhIn$_5$ from the C/T of Fig. 3(a). The magnetic entropy as a function of temperature is obtained by integrating C_e/T over T. The inset of Fig. 3(b) shows the temperature dependence of the magnetic entropy recovered per magnetic ion. The entropy is normalized by $(1 - x_{Gd})R \ln 2$ to account for the Ce contribution from the ground-state doublet and by $x_{Gd}R \ln 8$ to account for the Gd contribution ($J = 7/2$). In

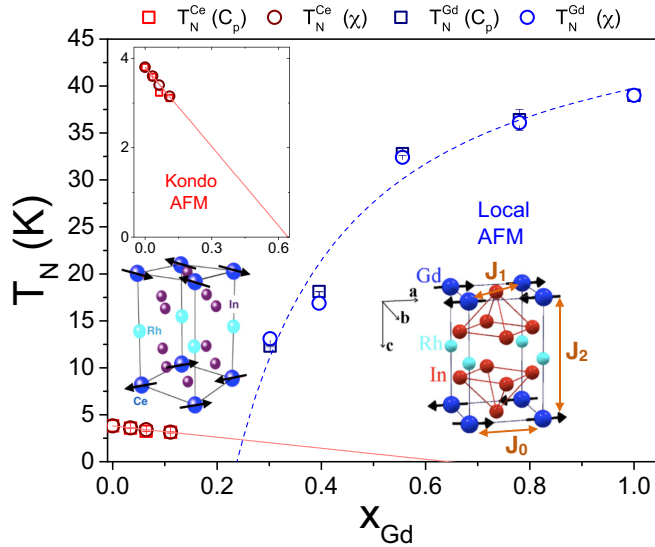FIG. 4. T-x phase diagram of the series $Ce_{1-x}Gd_xRhIn_5$.

pure $CeRhIn_5$, the magnetic entropy increases with increasing temperature and displays a kink at T_N. The total entropy recovered at T_N is only 30% of $R\ln 2$, suggesting a partially Kondo-compensated ordered moment. At low Gd concentrations, the moment is still partially compensated, although there is a slight increase in the recovered entropy below T_N as Gd is introduced into the lattice. As the Gd concentration is increased further, the entropy recovered at T_N becomes very close to the value expected for $J = 7/2$. This result corroborates our claim that below about 20% Gd, the magnetic order is dominated by the Ce Kondo lattice, whereas Gd^{3+} order dominates above this threshold.

Figure 4 summarizes our results in a T-x phase diagram. The series $Ce_{1-x}Gd_xRhIn_5$ displays two distinct regimes. The first one, at low Gd concentrations, reveals a linear decrease of T_N with x_{Gd}, similar to its La counterpart in which La is responsible for a Kondo hole in the system via dilution. Simple site dilution also should produce a linear decrease in T_N, which could be realized if, at dilute Gd concentrations, the ($S = 7/2$, $L = 0$) Gd moments did not interact with each other or with the Ce moments. Gd^{3+}, with a localized $4f$ level well below the Fermi energy, also may create a Kondo hole in Gd-doped $CeRhIn_5$, but this possibility remains to be

established unambiguously. In the case of $Ce_{1-x}La_xRhIn_5$, T_N extrapolates to $T = 0$ at a critical concentration of $x_c \sim 40\%$, which is the percolation limit of the 2D lattice. As shown in Fig. 4 and its inset, a linear extrapolation of Ce-derived magnetic order in $Ce_{1-x}Gd_xRhIn_5$ gives a larger x_c of ~63%, which is close to the percolation limit of the 3D lattice.

The quasi-2D crystal structures are identical for nominally isoelectronic $Ce_{1-x}La_xRhIn_5$ and $Ce_{1-x}Gd_xRhIn_5$, but the apparent magnetic dimensionality of Ce-derived order is increased with Gd dilution relative to La substitution. This is rather surprising and reflects a special role of the Gd^{3+} ions ($L = 0$, $S = 7/2$) in tuning the magnetic anisotropy of $CeRhIn_5$.

IV. CONCLUSIONS

In summary, we synthesize single crystals of $Ce_{1-x}Gd_xRhIn_5$ using the In-flux technique. Dilution at the Ce site in $CeRhIn_5$ by nonmagnetic La, Ising-like Nd, and Heisenberg-like Gd produce very different responses. Here, we show that a qualitative role of Gd substitution at low concentrations is to tune the high-temperature magnetic anisotropy in $CeRhIn_5$ to become isotropic with increasing Gd content. Naively, decreasing magnetic anisotropy could be consistent with an extrapolated 3D-like percolation limit for Ce-derived magnetic order in $Ce_{1-x}Gd_xRhIn_5$. This limit, however, is obtained from an extrapolation at low Gd concentrations where the magnetic susceptibility is still anisotropic and crystal-field effects are present. At these low Gd concentrations, Gd moments do not act as free paramagnetic impurities even in $La_{0.98}Gd_{0.02}RhIn_5$. Understanding why this is the case could be a first step in understanding the $Ce_{1-x}Gd_xRhIn_5$ phase diagram. More generally, the work presented here demonstrates the utility of substitution studies for revealing unexpected behaviors in correlated electron systems, such as the heavy-fermion antiferromagnet $CeRhIn_5$.

ACKNOWLEDGMENTS

[1] K. V. Klitzing, G. Dorda, and M. Pepper, Phys. Rev. Lett. **45**, 494 (1980).

[2] A. V. Balatsky, I. Vekhter, and J.-X. Zhu, Rev. Mod. Phys. **78**, 373 (2006).

[3] A. A. Abrikosov and L. P. Gorkov, Zh. Eksp. Teor. Fiz. **39**, 1781 (1960) [Sov. Phys. JETP **12**, 1243 (1961)].

[4] D. C. Tsui, H. L. Stormer, and A. C. Gossard, Phys. Rev. Lett. **48**, 1559 (1982).

[5] M. Sato, Y. Kobayashi, S. C. Lee, H. Takahashi, E. Satomi, and Y. Miura, J. Phys. Soc. Jpn. **79**, 014710 (2010).

[6] F. Hammerath, P. Bonfá, S. Sanna, G. Prando, R. De Renzi, Y. Kobayashi, M. Sato, and P. Carretta, Phys. Rev. B **89**, 134503 (2014).

[7] D. G. Mazzone, S. Raymond, J. L. Gavilano, E. Ressouche, C. Niedermayer, J. O. Birk, B. Ouladdia, G. Bastien, G. Knebel, D. Aoki, G. Lapertot, and M. Kenzelmann, Sci. Adv. **3**, e1602055 (2017).

[8] P. F. S. Rosa, J. Kang, Yongkang Luo, N. Wakeham, E. D. Bauer, F. Ronning, Z. Fisk, R. M. Fernandes, and J. D. Thompson, Proc. Natl. Acad. Sci. U.S.A. **114**, 5384 (2017).

[9] S. Raymond, S. M. Ramos, D. Aoki, G. Knebel, V. P. Mineev, and G. Lapertot, J. Phys. Soc. Jpn. **83**, 013707 (2014).

[10] J. Kondo, Prog. Theor. Phys. **32**, 37 (1964).

[11] G. R. Stewart, Rev. Mod. Phys. **56**, 755 (1984).

[12] H. Hegger, C. Petrovic, E. G. Moshopoulou, M. F. Hundley, J. L. Sarrao, Z. Fisk, and J. D. Thompson, Phys. Rev. Lett. **84**, 4986 (2000).

[13] P. G. Pagliuso, N. O. Moreno, N. J. Curro, J. D. Thompson, M. F. Hundley, J. L. Sarrao, Z. Fisk, A. D. Christianson, A. H. Lacerda, B. E. Light, and A. L. Cornelius, Phys. Rev. B **66**, 054433 (2002).

[14] E. D. Bauer, Yi-feng Yang, C. Capan, R. R. Urbano, C. F. Miclea, H. Sakai, F. Ronning, M. J. Graf, A. V. Balatsky, R. Movshovich, A. D. Bianchi, A. P. Reyes, P. L. Kuhns, J. D. Thompson, and Z. Fisk, Proc. Natl. Acad. Sci. U.S.A. **108**, 6857 (2011).

[15] P. F. S. Rosa, A. Oostra, J. D. Thompson, P. G. Pagliuso, and Z. Fisk, Phys. Rev. B **94**, 045101 (2016).

[16] W. Bao, P. G. Pagliuso, J. L. Sarrao, J. D. Thompson, Z. Fisk, J. W. Lynn, and R. W. Erwin, Phys. Rev. B **62**, R14621(R) (2000).

[17] S. Chang, P. G. Pagliuso, W. Bao, J. S. Gardner, I. P. Swainson, J. L. Sarrao, and H. Nakotte, Phys. Rev. B **66**, 132417 (2002).

[18] R. Lora-Serrano, D. J. Garcia, D. Betancourthc, R. P. Amaral, N. S. Camilo, E. Estévez-Rams, L. A. Ortellado G. Z., and P. G. Pagliuso, J. Magn. Magn. Mater. **405**, 304 (2016).

[19] T. Park, F. Ronning, H. Q. Yuan, M. B. Salamon, R. Movshovich, J. L. Sarrao, and J. D. Thompson, Nature (London) **440**, 65 (2006).

[20] E. Granado, B. Uchoa, A. Malachias, R. Lora-Serrano, P. G. Pagliuso, and H. Westfahl, Jr., Phys. Rev. B **74**, 214428 (2006).

[21] S. Doniach, Phys. B (Amsterdam, Neth.) **91**, 231 (1977).